Temporal Boundary Solitons and Extreme Superthermal Light Statistics

Chunhao Liang,[1,2] Sergey A. Ponomarenko,[2,3,*] Fei Wang,[4] and Yangjian Cai[1,4]
[1]Shandong Provincial Engineering and Technical Center of Light Manipulations & Shandong Provincial Key Laboratory of Optics and Photonics Devices, School of Physics and Electronics, Shandong Normal University, Jinan 250014, China
[2]Department of Electrical and Computer Engineering, Dalhousie University, Halifax, Nova Scotia B3J 2X4, Canada
[3]Department of Physics and Atmospheric Science, Dalhousie University, Halifax, Nova Scotia B3H 4R2, Canada
[4]School of Physical Science and Technology, Soochow University, Suzhou 215006, China

(Received 28 January 2021; accepted 28 June 2021; published 29 July 2021)

We discover the formation of a temporal boundary soliton (TBS) in close proximity of a temporal boundary, moving in a nonlinear optical medium, upon high-intensity pulse collision with the boundary. We show that the emergent TBS is unstable to perturbations caused by the cross-phase modulation between the TBS and the other soliton products of the collision and that such instability triggers colossal intensity fluctuations of the reflected pulse ensemble with unprecedented magnitudes of the normalized autocorrelation function for an even weakly fluctuating input pulse.

DOI: 10.1103/PhysRevLett.127.053901

Refraction and reflection of waves at a spatial interface separating two media with different refractive indices is a venerable subject. Because of the broken spatial translation symmetry, the spatial wave vector of a monochromatic wave, transmitted through the interface, changes, whereas the wave frequency remains the same. The picture is ubiquitous to waves of any physical nature, such as electromagnetic [1] or acoustic [2] waves. At the same time, the concept of time refraction, originally introduced in the context of photon acceleration in plasma physics [3], has only relatively recently percolated into optics and led to research into the fundamentals of the electromagnetic wave reflection and refraction at a temporal boundary [4–6] and optical pulse transmission through time-varying media [7–9].

Any temporal boundary (TB) breaks the time-translation symmetry causing a frequency change upon light transmission through the TB, hence the term photon acceleration. The light behavior at the TB, and in time-varying media in general, can be exploited to explore a multitude of fascinating fundamental phenomena in time domain, such as temporal total internal reflection [6], optical nonreciprocity [10,11], negative refraction [12], photonic topological insulators [13], photonic time crystals [14], and time reversal [15]; it can also open up a door to promising applications, including temporal waveguiding [8,16], frequency conversion [17], all-optical signal processing [18], and reconfigurable photonics [19,20]. In the nonlinear optics context, the weak probe pulse collision with a TB, generated by a strong pump pulse, for example, has been instrumental to simulate kinematical effects in gravitational physics [21–23] as well as to study soliton-TB interactions [24–27].

To the best of our knowledge, however, only the phenomena arising from bulk optical soliton interactions with the TB have been examined to date. In this Letter, we establish through extensive numerical simulations supported by asymptotic analysis that a temporal boundary soliton (TBS) can form in the vicinity of a TB moving in a nonlinear optical medium as an optical pulse of sufficiently high intensity, propagating in the medium, interacts with the TB. We show that the TBSs, being confined to the TB, propagate along the latter and are unstable to the perturbations induced by TBS interactions with bulk solitons via the cross-phase modulation. We further demonstrate that even modest intensity fluctuations of the input pulses trigger giant intensity fluctuations of light reflected from the boundary in an extremely rare scenario of an unperturbed TBS arriving at the observation plane $z = z_*$. The combination of these two discoveries is at the heart of extreme event generation in systems with nonlinear random waves confined to temporal boundaries. Our results reveal a novel, to our knowledge, mechanism of extreme event excitation in nonlinear wave systems with event horizons and establish a link between the two distinct research fields: (temporal) surface soliton theory and the physics of extreme events that has recently witnessed a flurry of research activity aiming to elucidate the fundamental physics behind the rogue wave formation [28,29].

We begin by examining optical pulse propagation in a generic weakly nonlinear medium with weak anomalous dispersion and a time-varying linear refractive index $n(t)$. We assume, for simplicity, that the time variation is encapsulated by a constant refractive index jump Δn propagating inside the medium at a constant speed v_b, that is, $n(t) = n_0 + \Delta n\theta(t - z/v_b - t_b)$, where $\theta(x)$ is a

Heaviside unit step function taking the value zero at $x < 0$ and unity at $x > 0$, and n_0 is a background linear refractive index of the medium [30]. The electric field $E(t, z)$ of a linearly polarized pulse can be expressed in terms of the slowly varying envelope $\Psi(t, z)$ and the carrier at frequency ω_0 as $E(t, z) = \Psi(t, z)e^{i(k_0 z - \omega_0 t)}$, where $k_0 = n_0\omega_0/c$ and we assume that $\Delta n \ll n_0$. In this approximation [31], the envelope evolution in the medium in the reference frame moving with the TB is governed by the modified nonlinear Schrödinger equation (NLSE) in the form

$$\partial_z\tilde{\Psi} + \frac{i\beta_2}{2}\partial_{\tau\tau}^2\tilde{\Psi} - ik_0\Delta n\theta(\tau - t_b)\tilde{\Psi} - i\gamma|\tilde{\Psi}|^2\tilde{\Psi} = 0. \quad (1)$$

Here $\tau = t - z/v_b$; $\beta_2 < 0$ and γ are anomalous group velocity dispersion and Kerr nonlinearity coefficients, respectively. We also introduced a gauge transformation viz., $\Psi = \tilde{\Psi}e^{i\nu\tau}$, where $\nu = -\Delta\beta_1/|\beta_2|$, $\Delta\beta_1 = \beta_1 - v_b^{-1}$ being an inverse group velocity mismatch between the pulse and TB, to remove a convective term associated with the group velocity mismatch.

We performed extensive numerical simulations solving Eq. (1) with a Gaussian input pulse, $\Psi(t, 0) = \sqrt{P_0}e^{-t^2/2t_p^2}$, having a fixed width $t_p = 0.6$ ps and variable input peak power P_0. In all our simulations we chose the group-velocity dispersion and nonlinearity parameters to be generic of a standard silica-glass fiber at the telecommunication wavelength, $\lambda_0 = 1.55$ μm: $\beta_2 = -0.02$ ps^2/m and $\gamma = 0.002$ W^{-1} m^{-1}. Further, we selected the TB parameters, $\Delta n = -0.787 \times 10^{-7}$ and $\Delta\beta_1 = 0.1$ ps/m so that the known condition [6] for the total internal reflection of the pulse at the TB with $t_b = 5$ ps in a linear medium, corresponding to $\gamma = 0$, is satisfied.

We exhibit representative results of our simulations in Fig. 1. As long as the input pulse power P_0 is relatively low, $P_0 = 80$ W, a soliton pulse travelling in a cloud of radiated waves—which exist due to nonintegrability of Eq. (1)—suffers (nearly) total internal reflection at the TB as most of the incident pulse energy is reflected back into $t < t_b$. This scenario is illustrated in Fig. 1(a1). As P_0 is increased to $P_0 = 250$ W, however, a multisoliton complex is formed on propagation of the input pulse toward the TB. The multisoliton complex suffers fission upon encountering the TB. A significant energy fraction of the multisoliton is concentrated near the TB and it self-induces a very deep and narrow waveguide via self-phase modulation; this is an emergent TBS. It follows that the TBS is transported as a sole mode of this self-induced waveguide as is displayed in Fig. 1(b1). We support our conjecture with a semiqualitative asymptotic analysis (see Supplemental Material [32] for details).

Another unambiguous signature of the localization of the discovered TBSs by the TB is revealed by their spectrum, exhibited in Figs. 1(a2)–1(d2) in terms of the relative frequency $\Omega = \omega - \omega_0$. In the spectral domain, the TBS emergence is heralded by the appearance of distinct

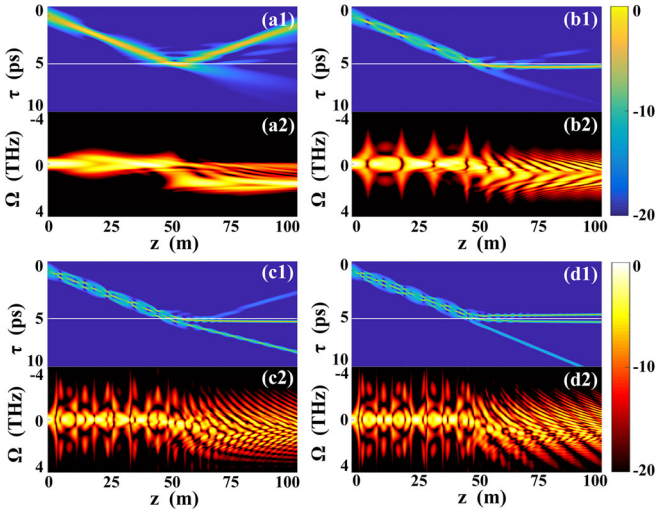

FIG. 1. Evolution of the intensity (a1)–(d1) and the spectrum (a2)–(d2) of an incident Gaussian pulse of width $t_p = 0.6$ ps and input peak power P_0: $P_0 = 80$ W (a1),(a2), $P_0 = 250$ W (b1),(b2), $P_0 = 593.8$ W (c1),(c2), and $P_0 = 709.4$ W (d1),(d2) as functions of the propagation distance z in the reference frame moving with the temporal boundary as the pulse propagates inside the nonlinear medium with the temporal boundary at $t_b = 5$ ps. The intensity and spectral distributions are displayed as functions of the time $\tau = t - z/v_b$ in the TB reference frame and the shifted frequency $\Omega = \omega - \omega_0$ relative to the carrier frequency ω_0 corresponding to the communication wavelength $\lambda = 1.55$ μm of a standard silica-glass fiber.

interference fringes that are clearly discernible on comparing Figs. 1(a2) and 1(b2). We attribute these fringes to spectral domain interference between the TBS and TB due to their close overlap in the time domain.

Further numerical simulations point to extreme sensitivity of TBS formation to the magnitude of the incident power P_0. Such a sensitivity is illustrated in videos 1 and 2 in the Supplemental Material [32] that show the incident multisoliton complex fission at the TB in the same P_0 range as that in Fig. 1(b1). We can infer from the videos as well as Fig. 1(b1) that only in a tiny range of P_0 are the conditions favorable to the TBS formation in the vicinity of the TB. In the vast majority of situations, the fission leads to bulk solitons and radiation waves carrying the energy away from the TB. The interaction between the TBS and the other fission products through the cross-phase modulation, neglected within the framework of our asymptotic analysis of Ref. [32], strongly influences the TBS dynamics along the TB and can trigger instability causing the temporal boundary soliton to detach from the TB and propagate away as a bulk soliton. We note that this interaction is, in general, more intricate than generic multisoliton interactions in homogeneous and inhomogeneous integrable systems [33].

As we increase the input peak power of the source pulse even further to $P_0 = 593.79$ W—see Fig. 1(c1)—the breakup of an incident multisoliton complex results in a

transmitted soliton, a weaker reflected soliton, and a TBS. All three strongly interact via the cross-phase modulation as is evidenced by the videos in Ref. [32]. Finally, as P_0 reaches 709.4 W, two TBSs can be simultaneously trapped in the same self-induced waveguide around the TB as is shown in Fig. 1(d1) for $\Delta n = -0.787 \times 10^{-7}$ and confirmed in video 4(c) of the Supplemental Material [32] for $\Delta n = -0.804 \times 10^{-7}$ and the source peak power in the range (715.8, 717.8 W) as well. This situation is quite delicate, however, as a two-boundary-soliton state, with the two TBSs symbiotically coexisting within the same self-induced waveguide by the TB, can swiftly disintegrate due to tiny fluctuations in P_0. This two-TBS breakup scenario is captured in videos 3 and 4 (Supplemental Material [32]). Figures 1(c2) and 1(d2) also depict a rather complex spectral interference pattern between the TBS, TB, and the other soliton fission products in this range of P_0.

We have discovered that the TBS instability triggers remarkable statistical anomalies if the source generates random input pulses. To reveal statistical signatures of TBS emergence, we examined an ensemble of 10^4 realizations of Gaussian input pulses of fixed width $t_p = 0.6$ ps and random input peak power, obeying Gaussian statistics with the probability density function (PDF) $\mathcal{P}(P_0) \propto e^{-(P_0-\langle P_0\rangle)^2/2\sigma_P^2}$. The PDF is completely determined by the mean peak power $\langle P_0\rangle$ and variance σ_P of the ensemble, where the angle brackets denote ensemble averaging. We remark that the Gaussian PDF of the source peak power is quite generic as it corresponds to an approximately Gaussian PDF of the soliton parameter, provided the fluctuations of P_0 are not too large (Supplemental Material [32]). Next, we constructed statistical ensembles with a given relative noise level in terms of the ratio of σ_P to $\langle P_0\rangle$. The source noise level ranges from 3%, to 10%, corresponding to weakly to moderately fluctuating pulses, respectively. We then evaluated the normalized intensity autocorrelation function, defined as [34]

$$g^{(2)}(\tau) = \langle |\Psi(\tau, z_*)|^4\rangle / \langle |\Psi(\tau, z_*)|^2\rangle^2, \tag{2}$$

in the observation plane at $z_* = 100$ m from the source.

We exhibit the results in Fig. 2 for weakly fluctuating (3% noise) ensembles with $\langle P_0\rangle$ taking on the values 80, 250, 593.8, and 709.4 W, corresponding, for simplicity, to the incident soliton fission scenarios displayed in Fig. 1 with the TB located at $t_b = 5$ ps. We can infer from the figures that at low $\langle P_0\rangle$, the global maximum of $g^{(2)}$ is on the order of unity, but as the TBS forms—see Fig. 1(b1)—the global maximum jumps up by an order of magnitude, reaching the magnitudes in excess of 40 for the ensemble with $\langle P_0\rangle = 250$ W. Thus, a dramatic increase in the magnitude of the maximum of the normalized intensity autocorrelation function signifies the TBS generation. Further increase in the average peak power leads to colossal

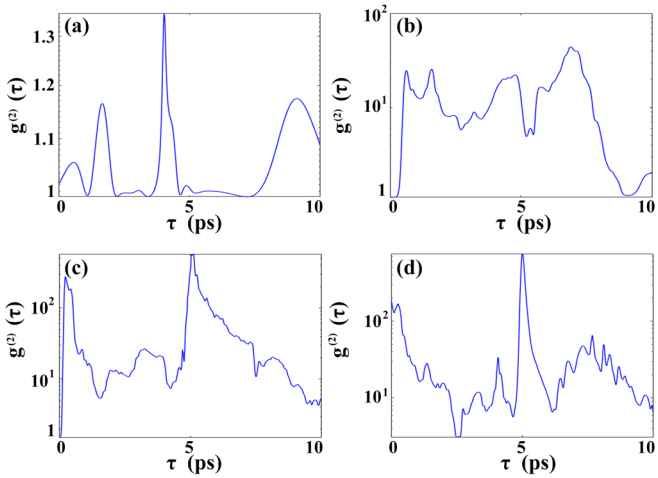

FIG. 2. Normalized intensity autocorrelation function of an ensemble of input Gaussian pulses with the average peak power at the source $\langle P_0\rangle$: $\langle P_0\rangle = 80$ (a), $\langle P_0\rangle = 250$ (b), $\langle P_0\rangle = 593.8$ (c), and $\langle P_0\rangle = 709.4$ W (d) as a function of time τ in the reference frame moving with the TB at $t_b = 5$ ps, evaluated at the receiver plane a distance $z_* = 100$ m away from the source.

intensity fluctuations encapsulated by $g^{(2)}$ attaining the values of nearly 600 and 800 in Figs. 2(c) and 2(d). In addition, as the average peak power of the source exceeds a certain threshold, around 600 W in our parameter regime, the shape of $g^{(2)}(\tau)$ changes qualitatively. In particular, a relatively broad $g^{(2)}$ distribution with the main peak past the TB, $\tau_{\max} > t_b = 5$ ps in Fig. 2(b) is superseded by an extremely tall and narrow spike centered around the TB, $\tau_{\max} \simeq t_b$ and sitting atop of a broad background distribution which is evident in Figs. 2(c) and 2(d).

We now elucidate the discovered statistical anomalies. First, the colossal intensity fluctuations associated with the TBS inception can be explained by revisiting the behavior of a single ensemble realization. As the realization (pulse) propagates inside the medium, a multisoliton complex forms, accompanied by some radiation on account of non-integrability of our modified NLSE. After a collision with the TB and subsequent soliton fission, in most cases the repulsion among the fission products inhibits the TBS formation. In these situations, the pulse arriving at the observation plane or receiver has a relatively low peak power. In rare cases, however, the TBS emerges and a very high peak power pulse arrives at the observation plane. Thus, denoting by N_{eff} ($N_{\text{eff}} \gg 1$) an effective number of realizations reliably reproducing the source ensemble statistics for a given noise level, we surmise that $\langle |\Psi|^2\rangle$ and $\langle |\Psi|^4\rangle$ at the position in the observation plane where the TBS arrives are dominated by a single ensemble realization Ψ_{TBS} corresponding to the case when the TBS is formed. It then follows at once that $\langle |\Psi|^2\rangle = N_{\text{eff}}^{-1} \sum_j |\Psi_j|^2 \simeq |\Psi_{\text{TBS}}|^2/N_{\text{eff}}$ and $\langle |\Psi|^4\rangle = N_{\text{eff}}^{-1} \sum_j |\Psi_j|^4 \simeq |\Psi_{\text{TBS}}|^4/N_{\text{eff}}$. Therefore, Eq. (2) implies that

$$g^{(2)}_{\max} \gtrsim N_{\text{eff}} \gg 1, \tag{3}$$

that is, giant magnitudes of the intensity autocorrelation function can be expected even for rather modest source noise levels.

To explain the pronounced growth of the global maximum of $g^{(2)}$ with $\langle P_0 \rangle$ for a given noise level, we recall that given the latter, our ensembles are constructed such that the variance of the source peak power PDF augments with $\langle P_0 \rangle$, making the source effectively noisier in terms of the peak power, and hence calling for a greater number of realizations N_{eff} to reproduce the source statistics. It then follows from Eq. (3) that the global maximum of $g^{(2)}$ must grow with $\langle P_0 \rangle$ as well.

Next, we refer to Fig. 3 from which the shape of $g^{(2)}(\tau)$ can be understood. The broad pedestal on which a huge spike of $g^{(2)}$ is situated for sufficiently large $\langle P_0 \rangle$ corresponds to the time interval of the receiver plane colored in gray in Figs. 3(a) and 3(c). This is the receiver time window where the TBS is likely to arrive after it has separated from the TB due to the cross-phase modulation induced instability. At the same time, the much shorter time interval, depicted in red in Fig. 3(c), contains the window in the neighborhood of t_b, where the TBS can arrive in a very

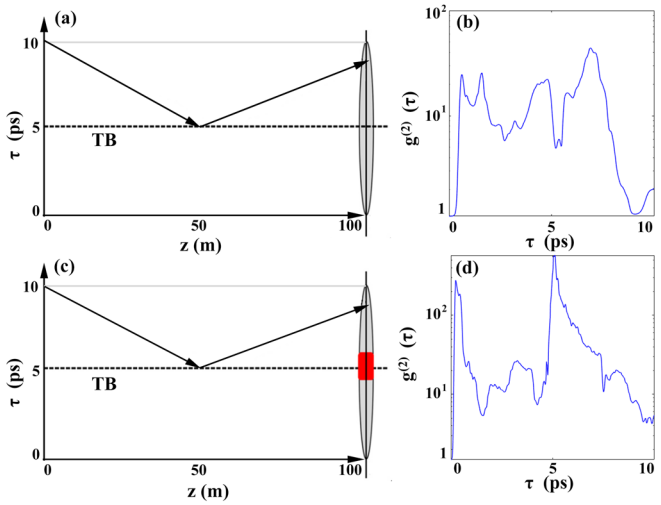

FIG. 3. Illustrating the shape of the normalized autocorrelation function. (a) The gray area corresponds to the time interval at the receiver where TBS and/or other soliton fission products are likely to arrive. (b) The broad normalized autocorrelation function $g^{(2)}(\tau)$, corresponding to a pulse ensemble with $\langle P_0 \rangle =$ 250 W and 3% noise level, evaluated at $z_* = 100$, exhibits a main peak and several secondary peaks of comparable magnitude. (c) The red area corresponds to the time interval at the receiver where exceptionally rare TBSs, which propagate all the way along the TB toward the receiver plane, arrive. (d) The normalized intensity autocorrelation function, corresponding to a pulse ensemble with $\langle P_0 \rangle = 593.8$ W and 3% noise level, evaluated at $z_* = 100$, features a tall and narrow spike residing on a broad pedestal comprised of a multitude of much lower peaks of comparable heights.

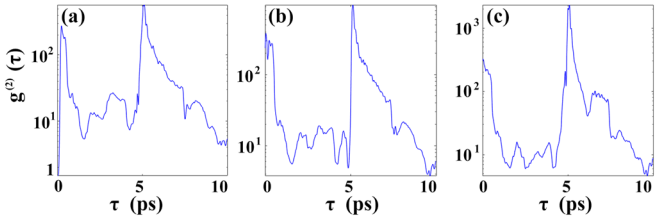

FIG. 4. Normalized intensity autocorrelation function of an ensemble of input Gaussian pulses with the average peak power at the source $\langle P_0 \rangle = 593.8$ W and 3% (a), 5% (b), and 10% (c) noise level as a function of time τ in the reference frame moving with the TB, evaluated at $z_* = 100$ m.

unlikely scenario that it is capable of traveling all the way along the TB toward the receiver, overcoming the overwhelming odds of having being peeled off of the TB through its interaction with the other (high-power soliton) fission products. This is an extremely rare event that can happen only for very high $\langle P_0 \rangle$, which explains the presence of the spike in Fig. 3(d) representing the ensemble with $\langle P_0 \rangle = 593.8$ W and its absence in Fig. 3(b) visualizing the ensemble with $\langle P_0 \rangle = 250$ W. Notice that the broad pedestal in Fig. 3(d) corresponds to the values of $g^{(2)}$ of the same order as those in Fig. 3(b).

Finally, we display in Fig. 4 the dependence of the intensity autocorrelation function on the noise level of the source for a given (high) average peak power of the input pulse ensemble, $\langle P_0 \rangle = 593.8$ W. It can be readily inferred from the figure that $g^{(2)}$ grows sharply as the source noise level is increased, attaining unprecedented, to our knowledge, magnitudes of 962 and 2327 for 5% and 10% noise levels, respectively. The revealed unprecedented values of $g^{(2)}$ exceed that of thermal light by more than 3 orders of magnitude. The precipitous growth of $g^{(2)}$ with the noise level can be qualitatively explained by recalling that one requires a larger number of ensemble realizations to faithfully reproduce a noisier ensemble, which, in turn, implies the increase of the maximum of $g^{(2)}$ by virtue of Eq. (3).

In conclusion, we stress that unlike previous studies concerned with either bulk soliton trapping by small defects, cf., [35], or generating bulk solitons upon ultrashort—in a femtosecond range—pulse fission at an optical even horizon [24–27] or with guiding weak pulses inside femtosecond soliton-induced waveguides [36], we have revealed temporal boundary soliton generation, such that the TBS guides itself along the TB inside a self-induced temporal waveguide in the optical medium. In addition, the observation of the predicted superthermal light statistics requires only picosecond pulses with modest input peak powers triggering no supercontinuum generation. We anticipate our results to contribute to a thriving multidisciplinary field of extreme event and rogue wave physics.

The authors acknowledge financial support from the Natural Sciences and Engineering Research Council of

Canada, (RGPIN-2018-05497); the National Natural Science Foundation of China (NSFC) (12004220, 11525418, 91750201, 11974218), China Postdoctoral Science Foundation (2019M662424), the National Key Research and Development Project of China (2019YFA0705000); the Innovation Group of Jinan (2018GXRC010), and the Local Science and Technology Development Project of the Central Government (No. YDZX20203700001766).

*serpo@dal.ca

[1] M. Born and E. Wolf, *Principles of Optics: Electromagnetic Theory of Propagation, Interference, and Diffraction of Light*, 7th expanded ed. (Cambridge University, Cambridge, England, 1999).
[2] P. M. Morse and K. U. Ingard, *Theoretical Acousitcs* (Princeton University Press, Princeton, NJ, 1986).
[3] J. T. Medonça, *Theory of Photon Acceleration* (Institute of Physics Publishing, Bristol, 2001).
[4] J. T. Medonça and P. K. Shukla, Time refraction and time reflection: Two basic concepts, Phys. Scr. **65**, 160 (2002).
[5] Y. Xiao, D. N. Maywar, and G. P. Agrawal, Reflection and transmission of electromagnetic waves at a temporal boundary, Opt. Lett. **39**, 574 (2014).
[6] B. P. Plansinis, W. R. Donaldson, and G. P. Agrawal, What is the Temporal Analog of Reflection and Refraction of Optical Beams?, Phys. Rev. Lett. **115**, 183901 (2015).
[7] Y. Xiao, G. P. Agrawal, and D. N. Maywar, Spectral and temporal changes of optical pulses propagating through time-varying linear media, Opt. Lett. **36**, 505 (2011).
[8] B. P. Plansinis, W. R. Donaldson, and G. P. Agrawal, Temporal waveguides for optical pulses, J. Opt. Soc. Am. B **33**, 1112 (2016).
[9] C. García-Meca, A. M. Ortiz, and R. L. Sáez, Supersymmetry in time domain and its applications in optics, Nat. Commun. **11**, 813 (2020).
[10] Z. Yu and S. Fan, Complete optical isolation created by indirect interband photonic transitions, Nat. Photonics **3**, 91 (2009).
[11] D. L. Sounas and A. Alù, Nonreciprocal photonics based on time modulation, Nat. Photonics **11**, 774 (2017).
[12] J. Pendry, Time reversal and negative refraction, Science **322**, 71 (2008).
[13] K. Fang, Z. Yu, and S. Fan, Realizing effective magnetic field for photons by controlling the phase of dynamic modulation, Nat. Photonics **6**, 782 (2012).
[14] E. Lustig, Y. Sharabi, and M. Segev, Topological aspects of photonic time crystals, Optica **5**, 1390 (2018).
[15] M. F. Yanik and S. Fan, Time Reversal of Light with Linear Optics and Modulators, Phys. Rev. Lett. **93**, 173903 (2004).
[16] J. Zhou, G. Zhang, and J. Wu, Comprehensive study on the concept of temporal optical waveguides, Phys. Rev. A **93**, 063847 (2016).
[17] Y. Zhou, M. Z. Alam, M. Karimi, J. Upham, O. Reshef, C. Liu, A. E. Willner, and R. W. Boyd, Broadband frequency translation through time refraction in an epsilon-near-zero material, Nat. Commun. **11**, 2180 (2020).
[18] S. Vezzoli, V. Bruno, C. DeVault, T. Roger, V. M. Shalaev, A. Boltasseva, M. Ferrera, M. Clerici, A. Dubietis, and D. Faccio, Optical Time Reversal from Time-Dependent Epsilon-Near-Zero Media, Phys. Rev. Lett. **120**, 043902 (2018).
[19] A. Kord, D. L. Sounas, and A. Alù, Magnet-less circulators based on spatiotemporal modulation of bandstop filters in a delta topology, IEEE Trans. Microwave Theory Technol. **66**, 911 (2018).
[20] L. Zhang, X. Chen, S. Liu, Q. Zhang, J. Zhao, J. Y. Dai, G. D. Bai, X. Wan, Q. Cheng, G. Castaldi, V. Galdi, and T. J. Cui, Space-time-coding digital metasurfaces, Nat. Commun. **9**, 4334 (2018).
[21] T. G. Phibin, C. Kuklewicz, S. Robertson, S. Hill, F. König, and U. Leonhardt, Fiber-optical analog of the event horizon, Science **319**, 1367 (2008).
[22] E. Rubino, F. Belgiorno, S. L. Cacciatori, M. Clerici, V. Gorini, G. Ortenzi, L. Rizzi, V. G. Sala, M. Kolesik, and D. Faccio, Experimental evidence of analogue Hawking radiation from ultrashort laser pulse filaments, New J. Phys. **13**, 085005 (2011).
[23] D. Faccio, Laser pulse analogies for gravity and analogue Hawking radiation, Contemp. Phys. **53**, 97 (2012).
[24] S. Robertson and U. Leonhardt, Frequency shifting at fiber-optical event horizons: The effect of Raman deceleration, Phys. Rev. A **81**, 063835 (2010).
[25] A. Demircan, S. Amiranashvili, and G. Steinmeyer, Controlling Light by Light with an Optical Event Horizon, Phys. Rev. Lett. **106**, 163901 (2011).
[26] A. Demircan, S. Amiranashvili, C. Brée, C. Mahnke, F. Mitschke, and G. Steinmeyer, Rogue events in the group velocity horizon, Sci. Rep. **2**, 850 (2012).
[27] E. Rubino, A. Lotti, F. Belgiorino, S. L. Cacciatori, A. Couaron, U. Leonhardt, and D. Faccio, Soliton-induced relativistic-scattering and amplification, Sci. Rep. **2**, 932 (2012).
[28] M. Onorato, S. Residori, U. Bertolozzo, A. Montina, and F. T. Arecchi, Rogue waves and their generating mechanisms in different physical contexts, Phys. Rep. **528**, 47 (2013).
[29] J. M. Dudley, G. Genty, A. Mussot, A. Chabchoub, and F. Dias, Rogue waves and analogies in optics and oceanography, Nat. Rev. Phys. **1**, 675 (2019).
[30] The emergence of temporal boundary solitons and anomalous superthermal light statistics in reflection from the temporal boundary does not depend on the steepness of the linear refractive index jump as we demonstrate in the Supplemental Material [32].
[31] G. P. Agrawal, *Nonlinear Fiber Optics*, 4th ed. (Academic Press, Amsterdam, 2007).
[32] See Supplemental Material at http://link.aps.org/supplemental/10.1103/PhysRevLett.127.053901 for the asymptotic theory of TBS, statistical ensemble formulation,

and videos of the incident pulse interaction with the temporal boundary.

[33] S. A. Ponomarenko and G. P. Agrawal, Nonlinear interaction of two or more similaritons in loss-and dispersion-managed fibers, J. Opt. Soc. Am. B **25**, 983 (2008).

[34] L. Mandel and E. Wolf, *Optical Coherence and Quantum Optics* (Cambridge University Press, Cambridge, England, 1995).

[35] X. D. Cao and B. A. Malomed, Soliton-defect collisions in the nonlinear Schrödinger equation, Phys. Lett. A **206**, 177 (1995).

[36] R. Driben, A. V. Yulin, A. Efimov, and B. A. Malomed, Trapping of light in solitonic cavities and its role in the supercontinuum generation, Opt. Express **21**, 19091 (2013).